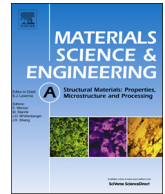




Contents lists available at ScienceDirect

Materials Science & Engineering A

journal homepage: www.elsevier.com/locate/msea

Improvement of high temperature mechanical properties of Ni-based oxide dispersion strengthened alloys by preferential formation of Y-Ti-O complex oxide

Chun Woong Park^a, Jong Min Byun^{b,*}, Won June Choi^a, Seung Yeung Lee^a, Young Do Kim^{a,*}

^a Department of Materials Science and Engineering, Hanyang University, 222 Wangsimni-ro, Seongdong-gu, Seoul 04763, Republic of Korea

^b Department of Materials Science and Engineering, Seoul National University of Science and Technology, Seoul 01811, Republic of Korea

ARTICLE INFO

Keywords:

ODS alloys
Mechanical alloying
High temperature properties
Complex oxide

ABSTRACT

Y_2O_3 is mainly applied as a dispersoid in Ni-based oxide dispersion strengthened (ODS) alloys. The added Y_2O_3 reacts with Ti and Al at a temperature above 1150 °C to form a complex oxide such as Y-Ti-O or Y-Al-O complex oxide. However, previous studies have shown that Y-Al-O complex oxide has relatively coarser particles than Y-Ti-O complex oxide.

In this study, Ti was first added to form Y-Ti-O complex oxide, which has relatively fine particles. Subsequently, Al was added to inhibit the formation of Y-Al-O complex oxide, thus improving the high-temperature mechanical properties of ODS alloys. Ni-based ODS alloy powders with composition Ni-15Cr-xTi-1.1 Y_2O_3 (without aluminum) were mechanically alloyed using a planetary mill. Thereafter, the mechanically alloyed powders were heat treated to form a complex oxide of Y-Ti-O. A second mechanical alloying was performed by adding 4.5 wt% Al to the heat treated powders. The products obtained after the second alloying were sintered by spark plasma sintering. The phase of the sintered specimens were analyzed using X-ray diffraction, their microstructures were analyzed by transmission electron microscopy and the size distribution of oxide particles was confirmed by image analysis. Moreover, the high-temperature mechanical properties of each composition were analyzed using a hot hardness tester.

1. Introduction

Ni-based oxide dispersion strengthened (ODS) alloys have a higher operating temperature and better high-temperature mechanical properties than conventional superalloys [1–6]. To further improve the mechanical properties of ODS alloys, size and dispersion of oxide particle are very important factors [7,8]. This is because according to the pinning effect, the dispersed oxide improves the mechanical properties of the alloy by inhibiting dislocation migration. This mechanism is more effective when the number of oxide particles per unit area is high and the distance between the particles is short [9]. Therefore, as fine oxide particles enhance the dispersion strengthening effect of ODS alloys, various studies on the refinement of oxide particle size have been conducted [10,11]. In general, Y_2O_3 is mainly applied as a dispersoid in ODS alloys. The added Y_2O_3 reacts with Ti and Al at a temperature above 1150 °C to form a complex oxide such as Y-Ti-O or Y-Al-O complex oxide, which have finer oxide particles than the initial Y_2O_3 . These complex oxides not only exhibit excellent high-temperature

stability but also process a large activation energy for diffusion, so that the growth of oxides is slow at high temperature and excellent properties are maintained for a long time [12]. It is well known that Y-Al-O complex oxide has coarser particles than Y-Ti-O complex oxide [13]. Therefore, the greater the quantity of Y-Ti-O complex oxide, the more the properties of the alloy are improved. In particular in the existence of coarse oxide particles with size of 100 nm or more, dislocations are concentrated to induce cracking, thereby degrading the properties of the ODS alloys [14].

In this study, to improve the high-temperature mechanical properties of Ni-based ODS alloys by the preferential formation of Y-Ti-O complex oxide, which has relatively fine particles, a two-stage process was applied. In the first stage, a powder with a composition of Ni-15Cr-xTi-1.1 Y_2O_3 (without Al) was alloyed using a planetary mill. After mechanical alloying, the powder was heat treated to form Y-Ti-O complex oxide. In the second stage, 4.5 wt% Al was added to the heat treated powder, and a second milling was performed. The mechanically alloyed powder was then sintered by spark plasma sintering. The

* Corresponding authors.

E-mail addresses: byun@seoultech.ac.kr (J.M. Byun), ydkim1@hanyang.ac.kr (Y.D. Kim).

<https://doi.org/10.1016/j.msea.2018.10.004>

Received 6 July 2018; Received in revised form 13 September 2018; Accepted 2 October 2018

Available online 09 October 2018

0921-5093/ © 2018 Elsevier B.V. All rights reserved.

sintered specimens were analyzed phase, oxide particles size and high-temperature mechanical properties.

2. Materials and method

2.1. Powders

Ni elemental powders has a purity of 99.9% and the size less than 63 μm . Cr powders has a 99.9% purity and an average size of 43 μm . Al powder has 99.9% purity and the size less than 30 μm . Ti powder has 99.9% purity and size less than 45 μm . Y_2O_3 elemental powder has 99.97% purity and average size of 20 nm. Ni, Al and Ti powders were produced by Kojundo chemical. Cr and Y_2O_3 powders were produced by RND Korea.

2.2. Power process by mechanical alloying and sintering

In this study, based on the commercial Ni-based ODS alloy, MA 6000, the basic composition was set to Ni-15Cr-4.5Al-2.5Ti-1.1 Y_2O_3 (wt %) and powders of each element were used. To form Y-Ti-O, which has fine particles, the powders were mechanically alloyed without Al and subjected to heat treatment. The mechanical alloying was performed using a planetary mill (PM 400, Retsch technology GmbH) at a ball-to-powder ratio of 10:1, and rotation speed of 200 rpm in Ar atmosphere for 20 h. Also, considering the reaction with the Ni matrix, the amount of Ti added was set to 5.0 wt%. In addition, specimens containing 2.5 and 7.5 wt% Ti, were prepared to confirm the effect of Ti concentrations. The detailed compositions are shown in Table 1. The Mechanically alloyed powder was heat treated at 1150 $^\circ\text{C}$ for 1 h in Ar atmosphere to form complex oxides. The heat treated powder was analyzed by XRD to confirm the formation of Y-Ti-O complex oxides. Al was then added to the mechanically alloyed powder, and a second milling was performed for 20 h under same conditions as the first stage milling. The mechanically alloyed powder was then sintered by spark plasma sintering (SPS 1050, Sumitomo Coal & Mining Ltd.). Spark plasma sintering (SPS) consolidation was performed in a vacuum condition at 1150 $^\circ\text{C}$, for 30 min under a peak uniaxial pressure of 50 MPa.

2.3. Analysis

The phases of mechanically alloyed powder, heat treated powder and sintered specimens were investigated using X-ray diffractometer (XRD, D/MAX 2500, RIGAKU) with Cu K α radiation of 0.1542 nm generated at 40 kV. The sintered specimens were polished mechanically to 0.03 mm, and punched. And then, they were polished electrically at 25 $^\circ\text{C}$ at 15 V and 0.5 A. 20% perchloric acid (HClO_4) and 80% acetic acid (CH_3COOH) were used as electrolytic solution [11]. The microstructures were analyzed by transmission electron microscopy (TEM, Tecnai F20 G2, FEI) and the size distribution of the oxide particles was confirmed by image analysis. The hot hardness value were also measured using a hot hardness tester (AVK-HF, Mitutoyo Co.) to confirm the changes in the high-temperature mechanical properties depending on the preferential formation of Y-Ti-O complex oxide.

Table 1
Composition of Ni-based ODS samples.

Sample	Composition	Process
Standard	Ni-15Cr-4.5Al-2.5Ti-1.1 Y_2O_3	One-stage
S1	Ni-15Cr-2.5Ti-1.1 Y_2O_3 + 4.5Al	Two-stage
S2	Ni-15Cr-5.0Ti-1.1 Y_2O_3 + 4.5Al	Two-stage
S3	Ni-15Cr-7.5Ti-1.1 Y_2O_3 + 4.5Al	Two-stage

3. Results and discussion

3.1. phase analysis

The XRD pattern of the alloys after each process are shown in Fig. 1. The XRD patterns of the mechanically alloyed powder after preferential formation of Y-Ti-O is shown in Fig. 1(a). This Y-Ti-O complex oxide was confirmed $\text{Y}_2\text{Ti}_2\text{O}_7$ (PDF# 01-074-9631). According to this result, Y-Ti-O complex oxide was formed during the heat treatment. The XRD pattern of the sintered specimens after spark plasma sintering is shown in Fig. 1(b). In the one-stage process, which is the conventional process, Y-Al-O complex oxide had relatively intense peaks. These Y-Al-O complex oxides were confirmed $\text{Y}_4\text{Al}_2\text{O}_9$ (PDF# 00-014-475) and $\text{Y}_3\text{Al}_5\text{O}_{12}$ (PDF# 00-009-310). On the other hand, in the two-stage process, the peak intensity of Y-Al-O complex oxide was relatively low. However, it could be observed that Y-Al-O complex oxide was formed due to the deficiency of Ti in the specimen containing 2.5 wt% Ti. In addition, TiO_2 was formed in the specimen containing 7.5 wt% Ti.

3.2. Microstructure and particle distribution analysis

TEM analysis was performed to analyze the size of the oxide particles. Fig. 2 shows the oxide particle size analysis results. The results confirmed that oxide particles existed throughout the entire matrix, and that the oxide particles had a size of 100 nm or less. The TEM result of the alloy produced using the one-stage process is shown in Fig. 2(a); fine oxide particles with a size of 10 nm or less and coarse oxide particles with a size of several tens of nanometers were formed simultaneously. Also, the result for the specimen containing 2.5 wt% Ti are shown in Fig. 2(b); many coarse oxides particles were observed in the matrix. These result suggested that the reaction did not proceed sufficiently because Ti reacted with the Ni matrix during the first heat treatment process and Y-Al-O complex oxide was formed due to the reaction of residual Y_2O_3 with Al. The result for the specimen containing 5.0 wt% Ti are shown in Fig. 2(c); no coarse oxide particles were observed, and numerous fine oxide particles with a size of 10 nm or less were observed. Fig. 2(d) shows the result for the specimen containing 7.5 wt% Ti; some coarse oxide particles were present, but the most oxide particles were fine. This suggested that the coarse oxide particles produced in the 7.5 wt% Ti was TiO_2 , an oxide of Ti formed due to the presence of excess Ti [15].

Image analysis was performed to accurately analyze the size of the oxide particles using an ImageTool (IT) 2.0 program, and the results are shown in Fig. 3. The analytical results showed that the specimen containing 5.0 wt% Ti had the smallest average oxide particle size (Fig. 3(c)), which was in agreement with the TEM observations further, the remaining specimens showed trends similar to those observed in the TEM images. However, the average oxide particle size and standard deviation of the specimen subjected to the conventional one-stage process were the largest, and the specimen subjected to the two-stage process showed relatively fine and uniform oxide particle size distribution.

3.3. Hot hardness properties from 25 to 1000 $^\circ\text{C}$

Hot hardness analysis was performed to analyze the changes in mechanical properties due to the refinement of the oxide particle size. All sintered specimens measured by electronic densimeter (EW-300SG, Alfa Mirage) had a density of 99.5% or more, and the hardness of the specimens was measured from 25 to 1000 $^\circ\text{C}$ at 100 $^\circ\text{C}$ intervals. As a result of the hot hardness analysis shown in Fig. 4, it was confirmed that the hardness value slowly decreased with decreasing temperature from 25 to 600 $^\circ\text{C}$, however, the hardness decreased sharply at the temperature above 600 $^\circ\text{C}$. This was because strengthening mechanisms such as solid solution strengthening, work hardening and grain-boundary strengthening were only applicable at temperatures below

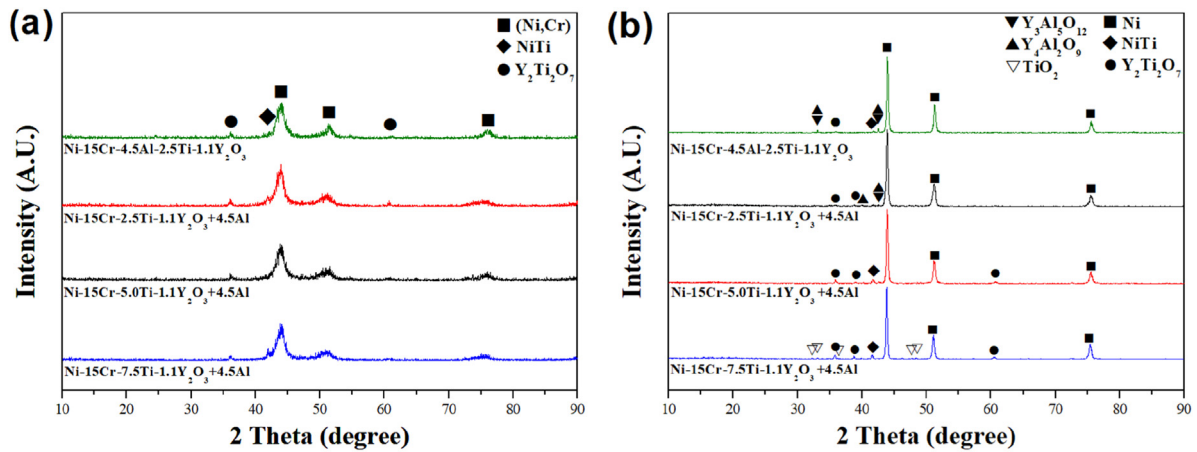


Fig. 1. XRD patterns of samples, (a) after heat treatment of Y-Ti-O formation and (b) after spark plasma sintering.

600 °C, above this temperature, the dispersion strengthening effect was the main mechanism [16]. Therefore, Ni-15Cr-5Ti-1.1Y₂O₃ + 4.5Al specimen, which had the finest particles, showed excellent mechanical properties, thus confirming that the properties degraded as the average size of the oxide particles increased. In addition, the hardness values of Ni-15Cr-4.5Al-2.5Ti-1.1Y₂O₃ specimen and Ni-15Cr-2.5Ti-1.1Y₂O₃ + 4.5Al specimen were relatively low at high temperatures, and the coarse particles caused dislocations rather than strengthening at high temperatures; their mechanical properties degraded.

4. Conclusion

In this study, we applied a two-stage process to Ni-based ODS alloys to suppress the formation of relatively coarse Y-Al-O complex oxides through the preferential formation of Y-Ti-O complex oxides. The effect of the refinement of the complex oxide particles on the high-temperature properties of Ni-based ODS alloys was analyzed.

1. In this study, 2.5, 5.0 and 7.5 wt% Ti were added to the Ni-based

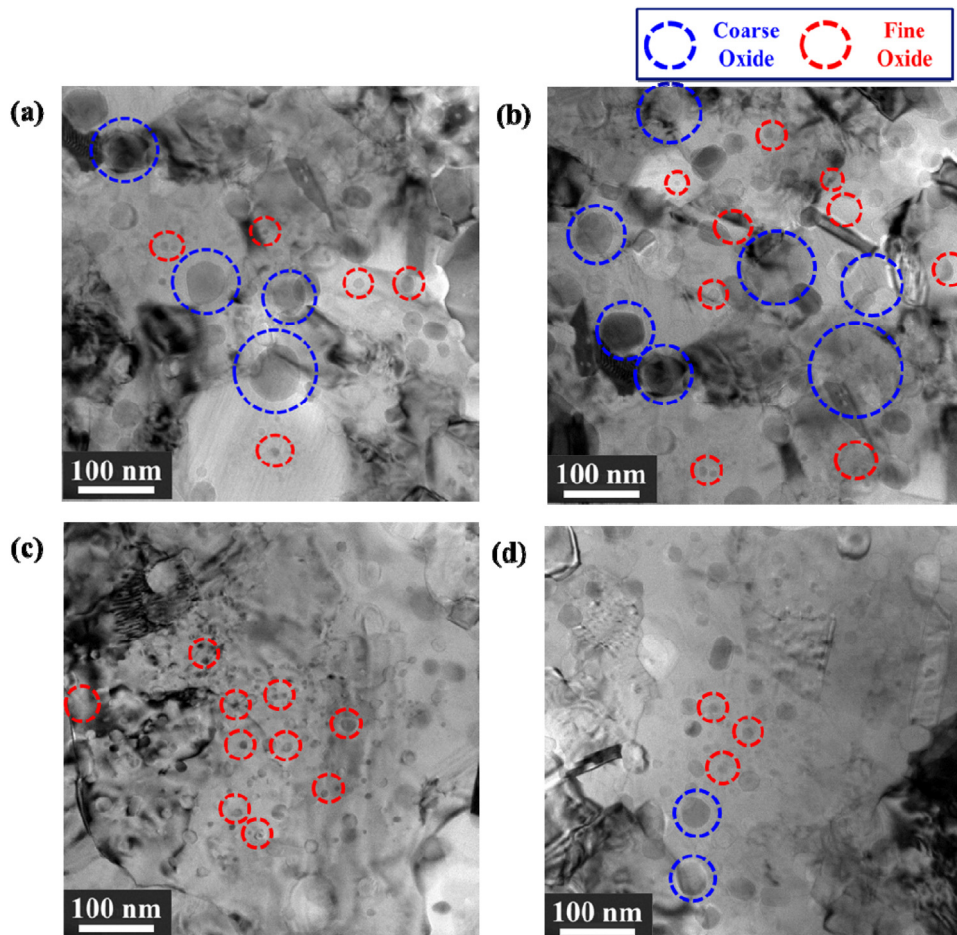


Fig. 2. TEM image of (a) Ni-15Cr-4.5Al-2.5Ti-1.1Y₂O₃, (b) Ni-15Cr-2.5Ti-1.1Y₂O₃ + 4.5Al, (c) Ni-15Cr-5.0Ti-1.1Y₂O₃ + 4.5Al, and (d) Ni-15Cr-7.5Ti-1.1Y₂O₃ + 4.5Al.

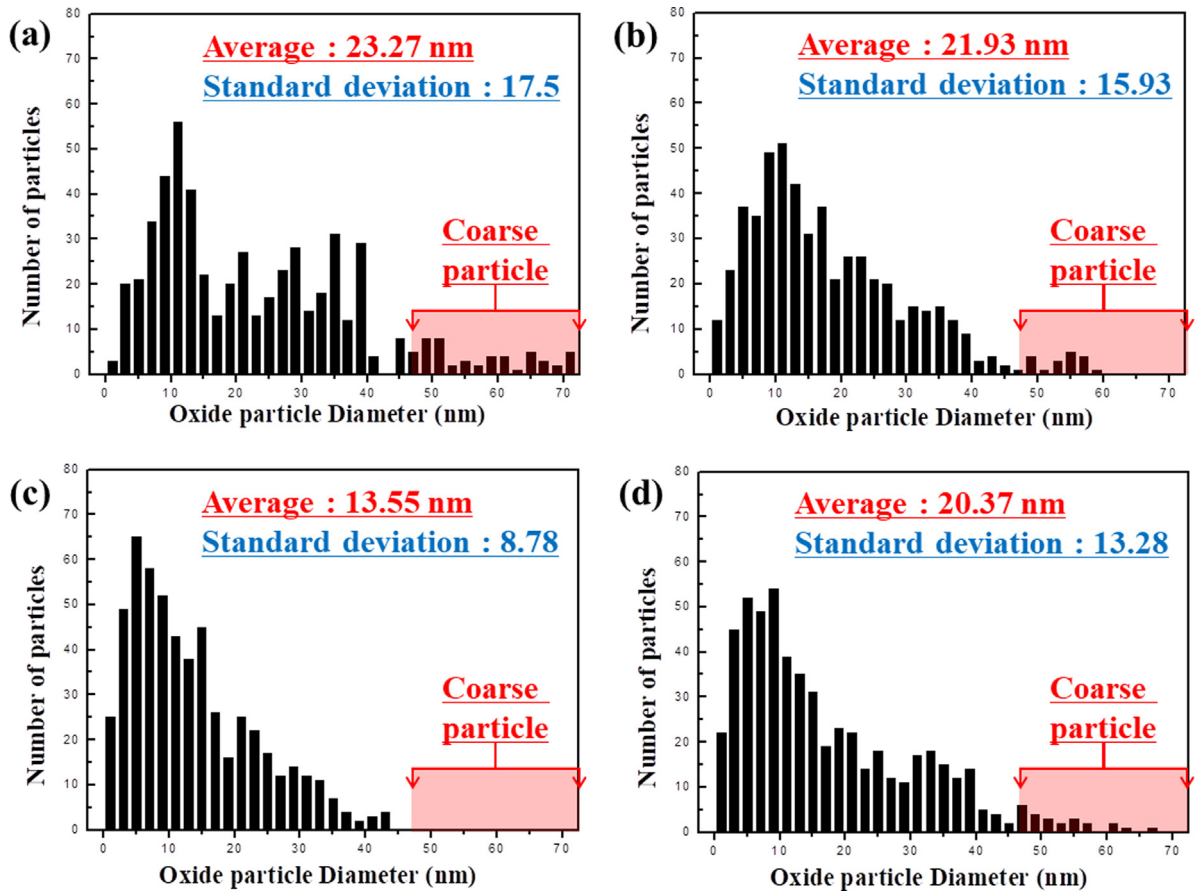


Fig. 3. Particle distribution of (a) Ni-15Cr-4.5Al-2.5Ti-1.1Y₂O₃, (b) Ni-15Cr-2.5Ti-1.1Y₂O₃ + 4.5Al, (c) Ni-15Cr-5.0Ti-1.1Y₂O₃ + 4.5Al, and (d) Ni-15Cr-7.5Ti-1.1Y₂O₃ + 4.5Al.

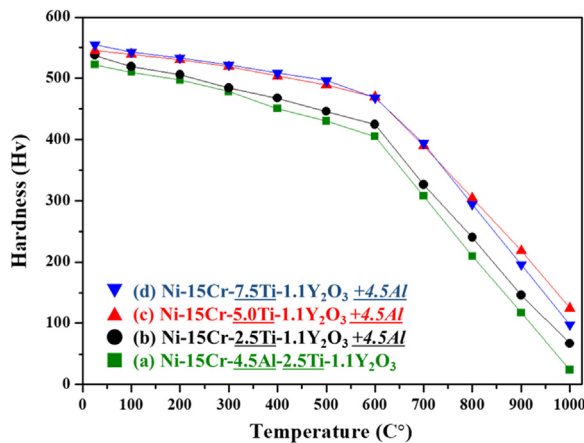


Fig. 4. Result of Vickers hardness test; (a) Ni-15Cr-4.5Al-2.5Ti-1.1Y₂O₃, (b) Ni-15Cr-2.5Ti-1.1Y₂O₃ + 4.5Al, (c) Ni-15Cr-5.0Ti-1.1Y₂O₃ + 4.5Al, and (d) Ni-15Cr-7.5Ti-1.1Y₂O₃ + 4.5Al.

ODS alloys. The obtained Ti-containing alloys were prepared by a two-stage process to ensure preferential formation of relatively fine Y-Ti-O complex oxide particles. Phase and microstructure analysis were then performed. The high-temperature mechanical properties of the prepared alloys were also analyzed.

- The phase analysis confirmed that Y-Ti-O complex oxide was preferentially formed by the two-stage process. The preferentially formed Y-Ti-O complex oxide existed even after the second mechanical alloying process. However, it was confirmed that TiO₂ was also formed in the specimen containing 7.5 wt% Ti.

- The TEM and image analysis showed that the specimen with subjected to the two-stage process contained finer oxide particle size distribution than that subjected to the conventional process. The specimen containing 5.0 wt% Ti exhibited the most fine and uniform distribution; in particular, no coarse oxide particles with 50 nm or more were observed.
- The high-temperature mechanical property analysis confirmed that the hardness of the produced through the preferential formation were superior to conventional method. In particular, the specimen containing 5.0 wt% Ti with the relatively most fine and uniform oxide particles showed best properties.

Acknowledgment

This research was supported by the Technology Innovation Program (10048158, Development of 980 °C grade superalloys strengthened by multi-component nano-oxides for commercialization of core materials in the field of the defense industry) funded by the Ministry of Trade, Industry and Energy (MI, Korea). This research was also supported by the Human Resources Program in Energy Technology of the Korea Institute of Energy Technology Evaluation and Planning (KETEP), granted financial resource from the Ministry of Trade, Industry & Energy, Republic of Korea (No. 20154030200900).

References

- J.R. Davis, *ASM speciality handbook: heat resistant materials*, ASM Speciality Handbook, ASM International, 1997.
- R.-W. Cahn, A.-G. Evans, M. McLean, *High-Temperature Structural Materials*, Chapman & Hall for The Royal Society, 1996.
- U. Glatzel, *Advanced High Temperature Alloys*, University Bayreuth, 2014.

- [4] J. Meyer, Advanced Gas Atomization Production of Oxide Dispersion Strengthened (ODS) Ni-base Superalloys through Process and Solidification Control (Graduate Theses and Dissertations), (2013).
- [5] D. Andy, R. Jones, Historical Perspective – ODS Alloy Development, University of Liverpool, 2010.
- [6] S.-M. Setted Aghamiri, H.-R. Shaverdi, S. Ukai, N. Oono, M. Nili Ahmadabadi, T. Okuda, Mater. Lett. 161 (2015) 568.
- [7] Q. Tang, T. Hoshino, S. Ukai, B. Leng, S. Hayashi, T. Wang, Mater. Trans. 51 (2010) 11.
- [8] S. Pasebani, A.K. Dutt, J. Burns, I. Charit, R.S. Mishra, Mater. Sci. Eng. A 630 (2015) 155.
- [9] N. Moelans, B. Blanpain, P. Wollants, Acta Mater. 55 (2007) 2173.
- [10] N. Oono, Q. Tang, S. Ukai, Mater. Sci. Eng. A 649 (2016) 250.
- [11] Q. Tang, S. Ukai, N. Oono, S. Hayashi, B. Leng, Y. Sugino, W. Han, T. Okuda, Mater. Trans. 53 (2012) 645.
- [12] H. Kishimoto, R. Kasada, O. Hashitomi, A. Kimura, J. Nucl. Mater. 386 (2009) 533.
- [13] G. Mengqiang, Z. Zhangjian, H. Helong, Z. Guangming, L. Shaofu, W. Man, J. Nucl. Mater. 462 (2015) 502.
- [14] C. Capdevila, M. Serrano, M. Campos, Mater. Sci. Technol. 30 (2014) 1655.
- [15] L. Barnard, N. Cunningham, G.R. Odett, I. Szlufarska, D. Morgan, Acta Mater. 91 (2015) 340.
- [16] A. Kelly, R.B. Nicholson, Strengthening Method in Crystal, John Wiley & Sons, Inc, New York, 1971.